

GT2004-53696

**THERMOMECHANICAL DESIGN OF A HEAT EXCHANGER
FOR A RECUPERATIVE AERO ENGINE**

Harald Schöenborn
MTU Aero Engines GmbH
Dachauer Strasse 665
D-80995 Muenchen, Germany
+49 89 1489 8326, +49 89 1489 99414
Harald.Schoenenborn@muc.mtu.de

Ernst Ebert
MTU Aero Engines GmbH
Dachauer Strasse 665
D-80995 Muenchen, Germany
+49 89 1489 3231, +49 89 1489 95338
Ernst.Ebert@muc.mtu.de

Burkhard Simon
MTU Aero Engines GmbH
Dachauer Strasse 665
D-80995 Muenchen, Germany
+49 89 1489 2651, +49 89 1489 6432
Burkhard.Simon@muc.mtu.de

Paul Storm
MTU Aero Engines GmbH
Dachauer Strasse 665
D-80995 Muenchen, Germany
+49 89 1489 6851, +49 89 1489 95340
Paul.Storm@muc.mtu.de

ABSTRACT

Within the framework programs of the EU for Efficient and Environmentally Friendly Aero-Engines (EEFEA) MTU has developed a highly efficient cross-counter flow heat exchanger for the application in intercooled recuperated aero-engines. This very compact recuperator is based on the profile tube matrix arrangement invented by MTU and one of its outstanding features is the high resistance to thermal gradients.

In this paper the combined thermomechanical design of the recuperator is presented. State-of-the-art calculation procedures for heat transfer and stress analysis are combined in order to perform a reliable life prediction of the recuperator.

The thermal analysis is based upon a 3D parametric finite element model generation. A program has been generated, which allows the automatic generation of both the material mesh and the boundary conditions. Assumptions concerning the boundary conditions are presented as well as steady state and transient temperature results.

The stress analysis is performed with a FEM code using essentially the same computational grid as the thermal analysis.

With the static temperature fields the static loading of the profile tubes is determined. From transient thermal calculations successive 3D temperature fields are obtained which enable the determination of creep life and LCF life of the part. Finally, vibration analysis is performed in order to estimate the vibration stress of the profile tubes during engine operation. Together with the static stress a Goodman diagram can be

constructed. The combined analysis shows the high life potential of the recuperator, which is important for economic operation of a recuperative aero-engine.

NOMENCLATURE

HPC high pressure compressor
LPC low pressure compressor
EGT Exhaust gas temperature
DP Pressure difference
Rm Ultimate tensile stress

INTRODUCTION

Current turbofan aero engines have reached a very high technology level. In order to further decrease fuel consumption and emission significantly new concepts are under investigation. MTU has developed the concept of an Intercooled Recuperative Aero-engine (IRA), which is shown in Fig. 1. A more detailed description can be found in references [1-3]. Between the LPC and HPC the air flows through an intercooler in the bypass duct. After the HPC the air is fed into the recuperator. The combination of these two components guarantees a high potential of fuel savings up to 20% against current aero-engines over a large speed range. Due to the weight constraints of the new components, the thermomechanical design of the recuperator is very important for the overall gain in efficiency of the complete engine.

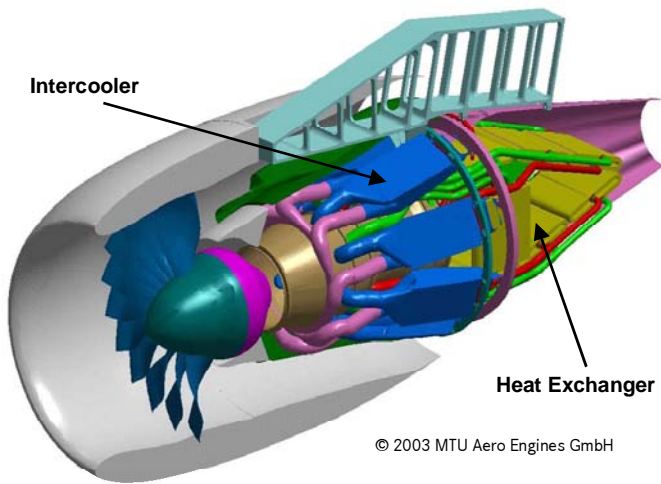


Figure 1: IRA - Intercooled Recuperative Aero-engine Concept

The basic design of the heat exchanger was developed by MTU some time ago, also for land based applications (references [4-9]). Special profiled tubes with a low aerodynamic loss and high heat transfer coefficients are used. Some new research is ongoing in order to further study the thermodynamics and aerodynamics of the matrix arrangement [10].

different U-shapes. Each profile tube is part of a tube set composed of either 4 or 3 profile tubes (see Fig. 3). A total of 3438 profile tubes are required for the heat exchanger. All parts of the heat exchanger are made of ALLOY625 except the wire-spacing and cushion wire-netting where INCO600 material is used.

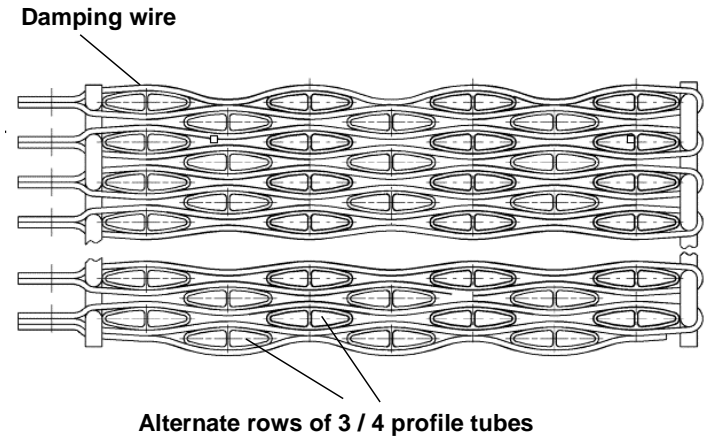


Figure 3: Profile tube matrix cross section

While the heat exchanger is in service the cushion wire-netting (woven metal fiber strips) damps the vibration and maintains the space between the profile tubes. To hold the system together wire-spacing is thread through the end of the cushion wire-netting. The U-shape of the matrix makes the recuperator resistant against thermal gradients.

A cover of sheet metal is placed around the matrix in order to stabilize the package and add some more damping to the system.

THERMAL ANALYSIS

Model

The thermal analysis task has concentrated first on the development of a finite element model of the matrix and second on both the prediction of steady state and transient temperature analysis. The finite element model has been developed in MSC/Patran. Rather than generating a single computational model of the hex geometry, it was decided to introduce flexibility into the model generation, so that future changes in the hex geometry could be easily facilitated in the thermal modeling. A program was written in the MSC programming language, PCL, which automatically generates a finite element model of the hex based on approximately 40 input parameters. These input parameters define the complete hex geometry, including overall dimensions, profile dimensions and spacing, as well as mesh parameters defining the fineness of the FE-mesh. In addition to the geometric parameters, some 15 parameters define the character of the flow, both on the air and gas sides of the hex, to facilitate the automatic generation of the advective and convective boundary conditions for the finite element model. More work was put into the development of this program than the generation of the single thermal finite element model would have required; however, the benefits of this additional effort are clear. Model generation can be

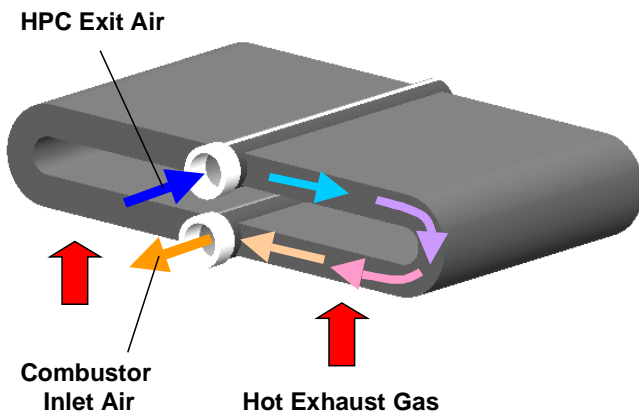


Figure 2: Recuperator

The heat exchanger consists of two manifold tubes (Fig. 2). The flow from the HPC enters the upper tube (distributor) from both sides and is distributed into the 3438 U-shaped profile tubes which are brazed into the manifold tubes and form the core of the matrix. The lower manifold tube (collector tube) collects the preheated air and leads it back to the combustion chamber. The hot exhaust gas from the low pressure turbine flows upwards through the matrix and is cooled down while heating up the air inside the profile tubes.

The matrix consists of 256 rows of profile tubes (Fig. 3). The profile tubes are folded from sheet metal and welded at their mating faces. Then the profile tubes are bent into the

accomplished quickly, the quality of the mesh is independent of the user, the program is extremely flexible in terms of the range of heat exchanger geometries which can be handled, and perhaps most importantly, future changes in the hex geometry can be rapidly accommodated.

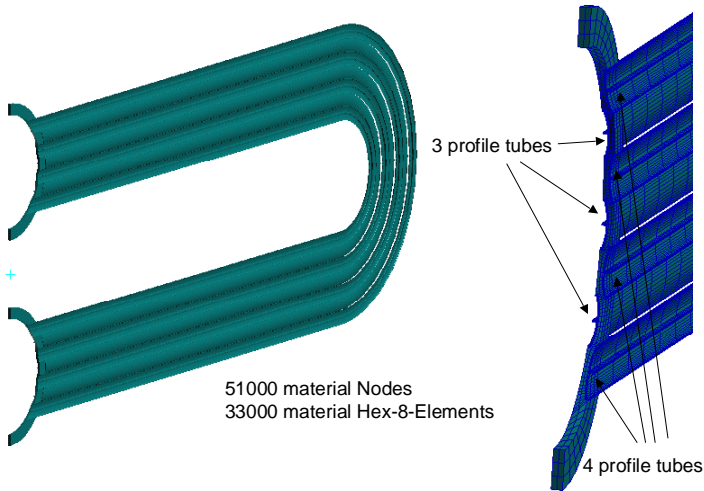


Figure 4: Thermal FE-mesh

The finite element model generated by the program is shown in Fig. 4. Due to symmetry conditions, the model need only consist of a single slice of the hex matrix, sliced through a row of three profile tubes on one side and four profile tubes on the other. Similarly due to symmetry conditions, only one side of the distributor and collector manifold walls are included in the model. Despite these simplifications arising from symmetry conditions, the model consists of approximately 51000 material nodes and 33000 material hex-8 elements.

Side	Property	Unit	End Take-Off	Max Climb	Avg. Cruise	Reverse
Air	Mass flow	[kg/s]	6.83	2.39	1.7	4.16
	Inlet pressure	[kPa]	3091	1084	760	1826
	Inlet temperature	[K]	722	597	507	608
Gas	Mass flow	[kg/s]	9.16	3.22	2.29	5.56
	Inlet pressure	[kPa]	166	55	39	125
	Inlet temperature	[K]	944	917	888	920

Table 1: Recuperator inlet conditions for the four primary performance points of the thermomechanical analysis

Boundary Conditions

Boundary conditions for the thermal analysis consist of fluid (air side and hot gas side) temperatures, mass flows and heat transfer coefficients. The advective flow network facilitates the determination of the local temperature boundary conditions. Inlet temperatures are specified at the two fluid nodes only, namely for air and gas inlet temperatures. With specified mass flow distributions, the temperature at all points in the advective systems are determined from an energy balance. Hence the temperature distributions in the advective systems become coupled to the material temperature distribution and are solved simultaneously.

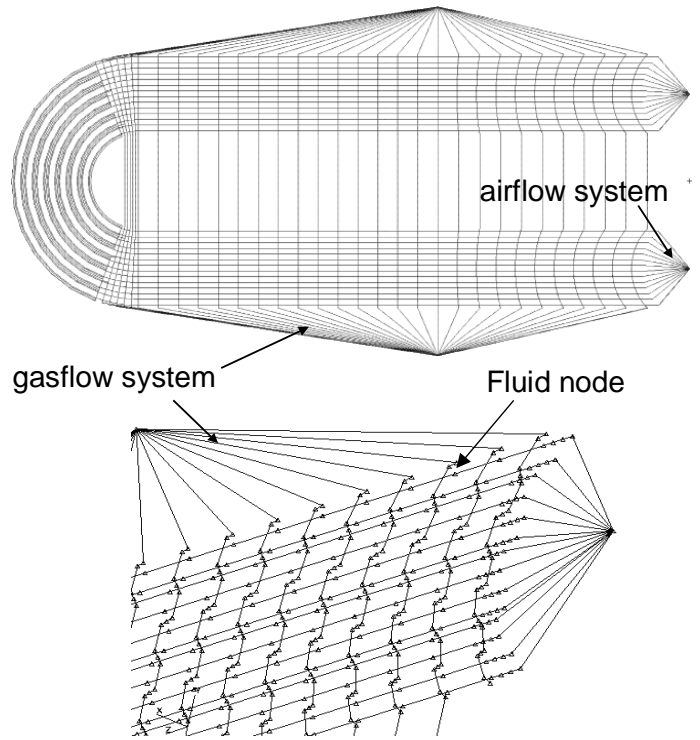


Figure 5: Advective flow network of the thermal model

In terms of the mass flow distributions, the following assumptions have been made: 1) the external hot gas flow is uniformly distributed along the length of the matrix, and 2) the mass flow on the air side from the distributor manifold into the profile tubes is taken to be inversely proportional to the length of the profile tube. The advective system is shown in Fig. 5. It consists of 2900 advective elements and 4500 fluid nodes.

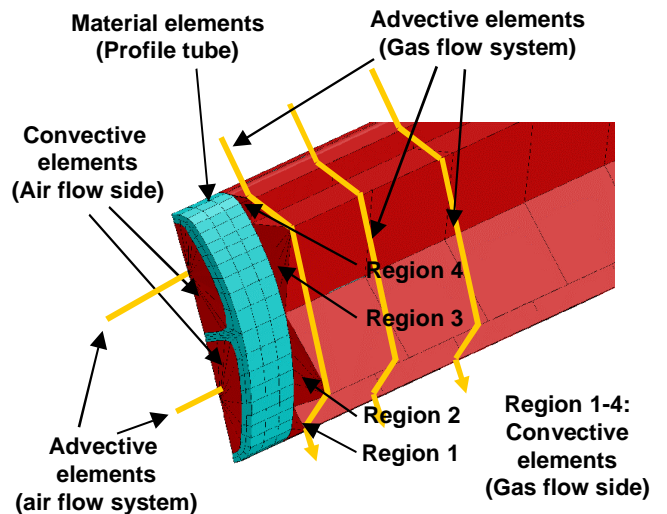


Figure 6: Interaction between advective flow network and material mesh at a profile tube

The inlet air and gas temperatures are based on the results of a 1D performance calculation of the aeroengine. The performance data at the recuperator inlet are given in Table 1 for the four principal load cases of the design mission. Typical deterioration increments, derived from a similar-sized non-intercooled, non-recuperated engine, are added to the inlet temperatures to simulate realistic operational conditions.

The heat transfer coefficients on the air side are determined by correlations for turbulent flow in ducts. For the gas side correlations for flow over tube bundles are used. The external surface of the profile tubes are divided into four regions, for which the heat transfer coefficients are determined. The regions are shown in Fig. 6. This figure also shows the interaction between the convective, the advective and the material elements.

Radiation is not accounted for in the model; however, at the temperature levels and temperature distribution encountered in the hex matrix, radiative heat transfer may be neglected.

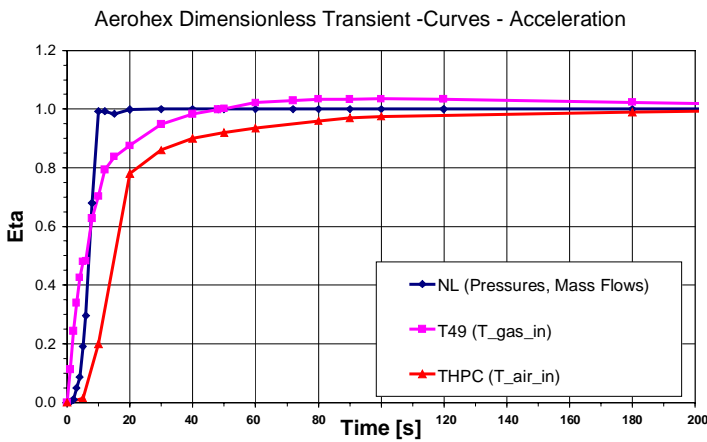


Figure 7: Non-dimensional transient behavior of boundary conditions during acceleration

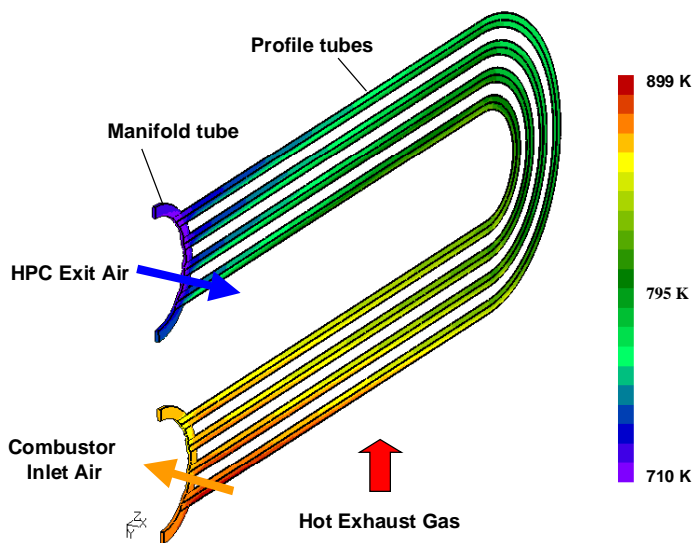


Figure 8: Temperature distribution at Take-Off conditions

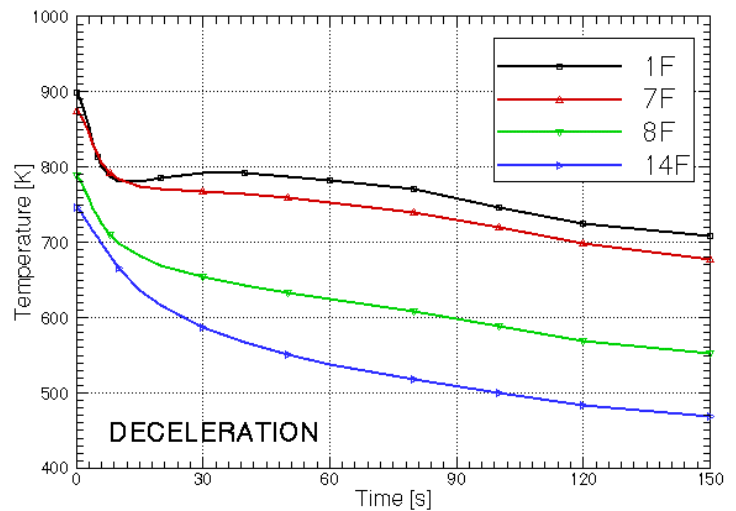
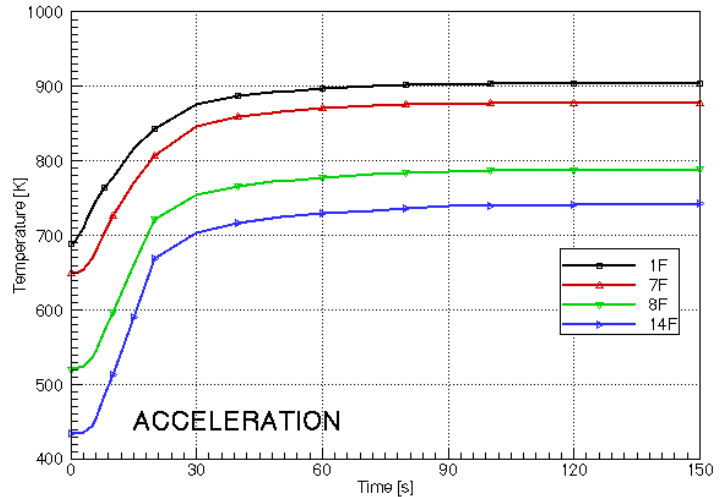
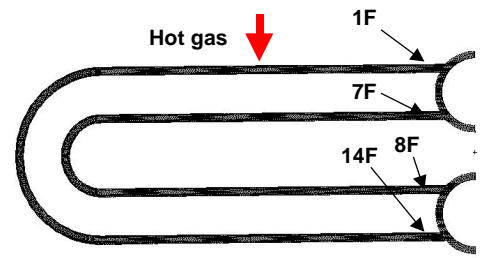


Figure 9: Transient temperature response at selected profile tube locations during minicycle

The entire mission profile is conservatively represented for purposes of an LCF life analysis by a minicycle, the first part representing the initial acceleration from idle to take-off conditions and climb to altitude, and the second part representing deceleration.

In undertaking a transient thermal analysis, the transient behavior of the boundary conditions, such as hex inlet temperatures and mass flows, during such acceleration and deceleration maneuvers must be known. The transient behavior of the boundary conditions was assumed from a conventional aero-engine of the same thrust class, but without intercooling or

recuperation, since no data from an IRA engine had been available. One would expect, as a result of the additional thermal inertia of an intercooler and recuperator, that the IRA would have a slower thermal transient response at the exhaust exit than a conventional engine of the same size. Hence the use of transient data from a conventional engine is justified as it would lead to conservative estimates of the LCF life. The transient behavior of the hex boundary conditions for the acceleration idle-takeoff, in the form of non-dimensional curves, are shown in Fig. 7 qualitatively. Similar curves exist for the deceleration from takeoff to ground idle, but are not reproduced in this paper.

Computational Results

Temperature calculations have been performed for different steady-state performance points such as ‘end take-off’ using the commercial program MSC/Thermal as solver. This program allows to incorporate user defined correlation, which are used for determination of the heat transfer coefficients, during an analysis run. The material temperature distribution at this point is shown in Fig. 8. Material temperatures in the hex are far from uniform, varying considerably not only along the length of the profile tubes, but also across the tube bundle. The peak temperature is found not surprisingly on the leading edge of the first profile tube, close to the collector manifold.

The transient temperature distribution was calculated for a minicycle ‘idle-takeoff-idle’. Transient temperature results are plotted in Fig. 9 for selected locations on the profile tubes. The shown material temperatures are selected close to the stagnation point of the profiles. As can be seen the heat up of the profile tubes at different locations is relatively homogeneous during the acceleration phase whilst the response curves during deceleration vary significantly. The temperature curves for the locations 1F and 7F cross one another during the first few seconds of the deceleration due to the latent heat of the profile tubes. While the tubes at the location 1F are exposed directly to the lower gas temperatures, the tubes at location 7F experience a delayed gas temperature reduction due to the above mentioned mechanism. A similar behavior is seen in the transients for locations 8F and 15F, but is not strong enough to cause a crossing of the temperature curves.

Since the first profile tube close to the collector manifold experiences the highest material temperatures and the fastest response curves during a transient change of the power setting, the region marked with ‘1F’ in Fig. 9 will be the most critical one of the hex tubes in terms of the matrix life.

STRUCTURE MECHANICAL ANALYSIS

The profile tubes with their thin wall thickness are the life determining parts of the recuperator. Thus, some effort has been made in order to perform an analytical life prediction of this part as up to now only little practical experience has been collected. ABAQUS was used as FEM code.

Model

In Fig. 10 a Finite-Element model of the matrix is shown. Due to symmetry conditions the model is reduced to one row with four profile tubes. Nevertheless, this model contains more than 150,000 nodes and 28,000 twenty-noded hexaeder elements. The damping wires are modeled as multi-point constraints between the profile tubes. The boundary conditions

at the symmetry plane of the manifold tubes were varied according to the type of analysis.

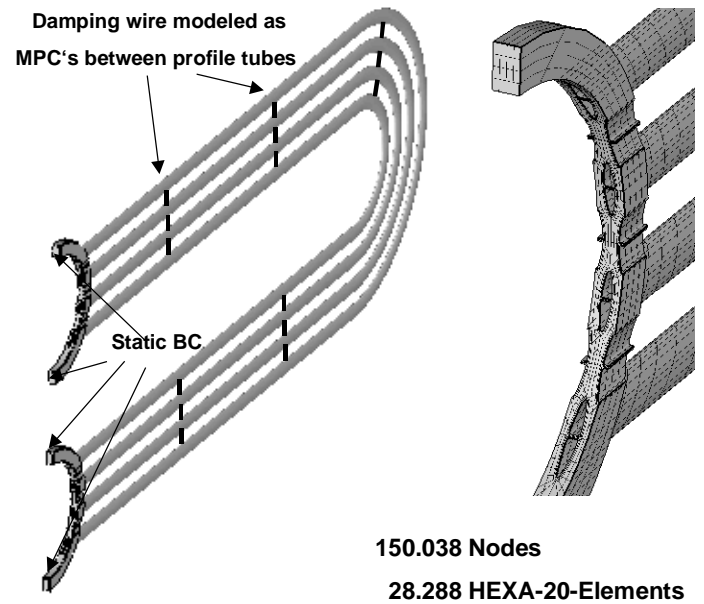


Figure 10: FE model structure mechanics

Static stress

Fig. 11 presents the stress results of an analysis with thermal load and internal pressure, which is applied as a distributed load onto the inner surface of the profile tubes and manifolds. Here, the static mean stress is determined, which is used later in the Goodman-diagram together with the results from the vibration analysis.

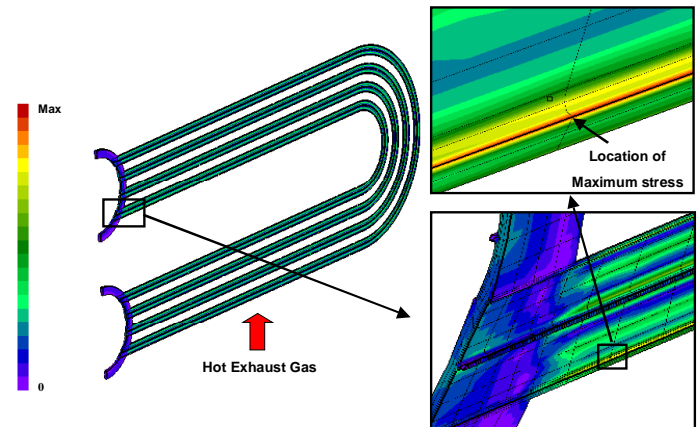


Figure 11: Static Mises Stress during Take-Off

Creep

A non-linear creep analysis was performed with a special creep user subroutine developed by MTU. A mission typical for a trans-atlantic flight was assumed. Fig. 12 shows the exhaust gas temperature and the internal profile tube pressure during the mission, made dimensionless with the maximum conditions (Take-off conditions).

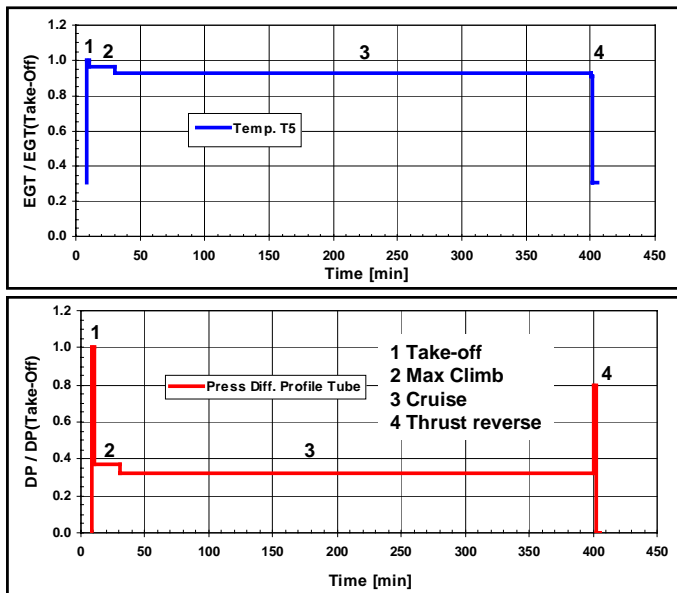


Figure 12: Mission temperature and pressure

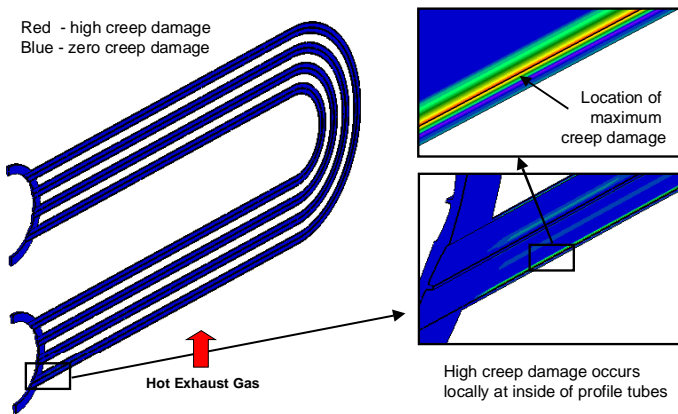


Figure 13: Example evaluation creep calculation

A large number of missions was considered and the time at each temperature level was summed up. For each condition of this mission, 3D temperature distributions were calculated.

The complete material creep curves for different temperatures are prepared and fed into the creep subroutine. Then for each time step the creep velocity is determined for each node using the Larson-Miller-Parameter and a differential creep strain is calculated. All these creep strains are summed up for each node yielding the creep strain distribution. Fig. 13 shows an example of such a result. It can be seen that only in the first row which is exposed to the hot exhaust gas at the inner small radius, where the stress due to internal pressure is highest, a considerable creep damage is accumulated. However, this creep damage did not exceed the limit of 1.0 for the assumed number of missions.

LCF

As the mission was appropriate for the creep simulation, for a complete LCF calculation too many time steps would have been necessary. Thus, as is usual only a mini-cycle as described above is considered. In Fig. 14 the Mises stress

results from this mini-cycle transient analysis is presented for the maximum stress location.

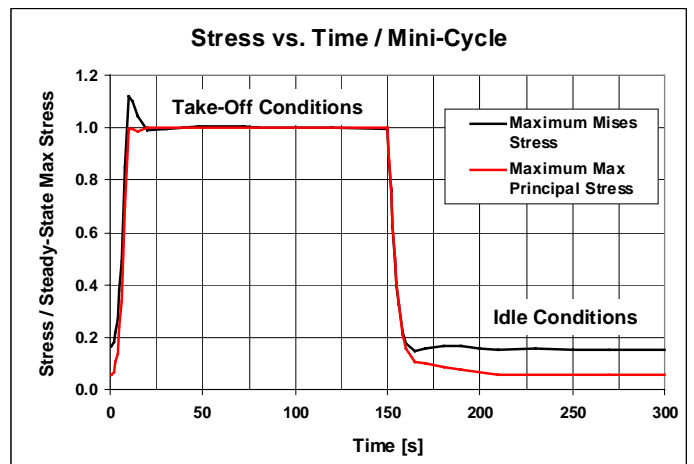


Figure 14: TMF Analysis Mini-cycle

It can be seen that there is only a small overshoot of about 10% in Mises stress during acceleration to take-off conditions against steady-state take-off conditions. The maximum principal stress did even show less overshoot. This is due to the U-shaped design of the profile tubes which result in this excellent thermomechanical behavior of the matrix.

Vibration

The basis for the vibration analysis is the determination of the eigenmodes of the profile tube package. Fig. 15 shows four eigenmodes out of the many hundreds of modes. Modes 1 and 4 are the first and second bending modes in the horizontal plane, where the matrix is relatively soft. These modes are not crucial as long as the matrix is limited in this direction by the side walls in the engine. Mode 3 is the first bending mode in vertical direction and is more dangerous due to nearly no geometrical constraints in this direction. All higher modes yield vibrations of single profile tubes against each other and are not considered as critical as the matrix is highly damped.

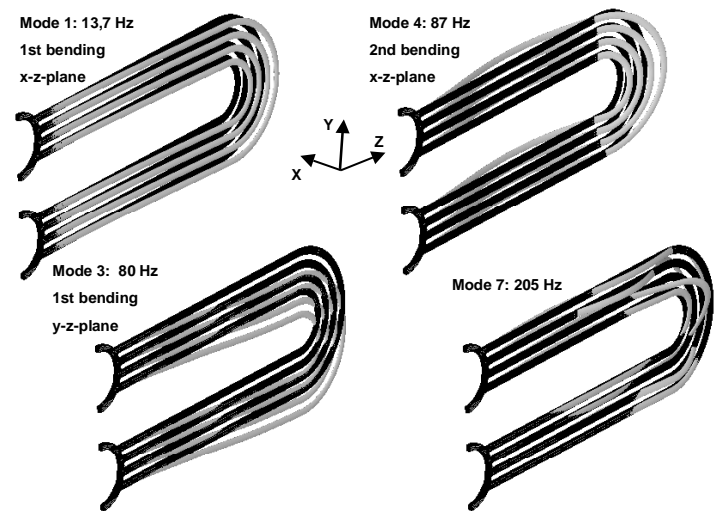


Figure 15: Some Eigenmodes

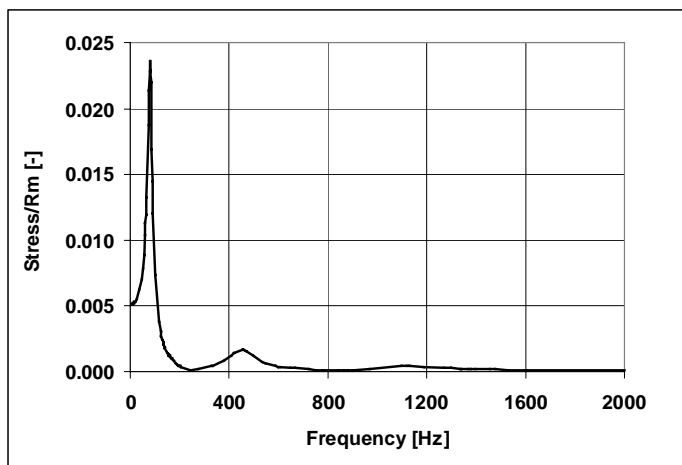


Figure 16: Stress response at 1g excitation at location of maximum stress (Mises)

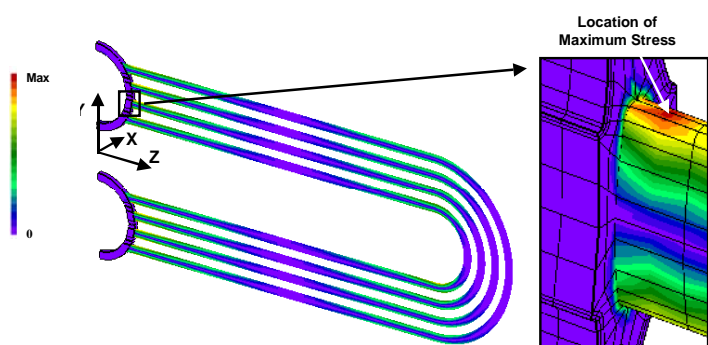


Figure 17: Vibration stress distribution

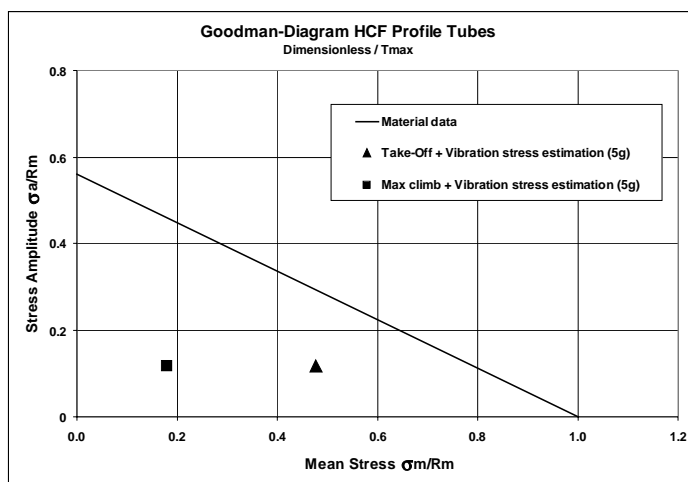


Figure 18: Goodman-diagram

A modal-based steady-state dynamic analysis was performed in the frequency range from 5 to 2000 Hz. A uniform 1-g excitation level was used with 10% of critical damping. Fig. 16 presents the Mises response stress (made dimensionless with R_m) of the location of maximum stress (see Fig. 17). The highest stresses occur for the first bending mode at 80Hz. At higher frequencies, the stress is much lower. Fig. 17 shows qualitatively the vibration stress distribution at 80Hz. Finally it is assumed that the matrix has a vibration excitation

of 5g. With this vibration stress amplitude and with the static stress determined previously a point can be drawn into the Goodman diagram (Fig. 18). It can be seen that for the take-off conditions there is still some safety margin against HCF failure. The experimental determination of vibration stress of a matrix on a shaker table and in a real engine with strain-gauges remains a very important point in order to verify the analytical predictions.

CONCLUSIONS

The thermomechanical procedure for the analytical life prediction of a recuperator for aero engines was presented. State-of-the-art calculation methods for thermal analysis and stress analysis were used. The analytical life prediction including a combination of LCF, creep and vibration has shown that the recuperator has a life potential as usually required for aero engines. The outstanding thermomechanical design makes this type of recuperator not only attractive for aero-engines, but also for other applications in power generation. The analytical analysis shows that there are still some margins to account for difficulties which may arise in the real engine (corrosion, vibration). Now this prediction has to be proven in practical use during future component and engine test programs.

ACKNOWLEDGMENTS

This work has been financially supported by the EU under the "Competitive and Sustainable Growth Programme" contract No G4RD-CT-1999-00069. The authors wish to thank the EU for supporting this program. The permission for publication is gratefully acknowledged.

REFERENCES

- [1] Broichhausen, K.; Scheugenpflug, H.; Mari, Ch.; Barbot, A., 2000, "CLEAN The European Initiative Towards Ultra Low Emission Engines, ICAS 2000, Harrogate, UK
- [2] Wilfert, G., Massé, B., 2001, "Technology integration in a low emission heat exchanger engine", Proceedings of the 8th CEAS European Propulsion Forum, Nottingham, UK
- [3] Scheugenpflug, H., Wilfert, G., Simon, B., 2001, "Erfüllung zukünftiger Umweltaforderungen durch den Einsatz eines Wärmetauschertriebwerks", DGLR-Jahrbuch Band 3, pp 1647 - 1654
- [4] Pellischek, G; Reile E., 1992, "Compact energy recovery units for vehicular gas turbines", SAE paper 920151
- [5] Pellischek, G, Kumpf, B., 1991, "Compact heat exchanger technology for aero engines", ISABE paper 91-7019
- [6] Eggebrecht, R., Schlosser, W., 1986, "Kompakter Hochtemperatur-Wärmetauscher für Wellenleistungsturbinen", MTZ Motortechnische Zeitschrift 47, 1986, pp235-241
- [7] Duffy, R. J., Hower, G. K., 1987, "Turbine propulsion for heavy armored vehicles", AIAA-paper 87-1911
- [8] Brockett, W., Koschier, A. V., 1992, "LV100 AIPS Technology - for future army propulsion", ASME-paper 92-GT-391
- [9] Koschier, A. V., Mauch, H. R., 1999, "Advantages of the LV100 as a power producer in a hybrid propulsion system for future fighting vehicles", ASME paper 99-GT-416
- [10] Goulas, A; Katheder, K.; Palikaras A.; Yakinthos, K., 2003, "Flow Measurements and Investigations in a Staggered Tube Matrix of a Heat Exchanger", Int. J. of Heat & Technology, Vol.21, n.2